

# Complex activation is more focal and concentrated to parenchymal tissue

D. B. Rowe<sup>1</sup>

<sup>1</sup>Department of Biophysics, Medical College of Wisconsin, Milwaukee, WI, United States

## Introduction:

In functional magnetic resonance imaging, voxel time courses after "image reconstruction" are complex valued. Nearly all fMRI studies derive functional "activation" based on magnitude-only data time courses [1]. The phase time courses are usually discarded. Recently a magnitude activation from complex data model was introduced that did not lose activation power as the SNR decreased [2].

## Model:

In a voxel, the observed complex-valued data can be described with the vector/matrix model

$$y = [(X\beta \cos \theta)', (X\beta \sin \theta)']' + \eta, \quad \eta \sim N(0, \sigma^2 I_{2n})$$

where the  $2n \times 1$  vector  $y = (y_R', y_I)'$  is the  $n \times 1$  vector of observed real components stacked on the  $n \times 1$  vector of observed complex components,  $X$  is the  $n \times (q+1)$  design matrix,  $\beta$  is the  $(q+1) \times 1$  vector of regression coefficients,  $\theta$  is the  $1 \times 1$  phase angle, and the vector  $\eta = (\eta_R', \eta_I)'$  is the  $n \times 1$  vector of real component errors stacked on the  $n \times 1$  vector of complex component errors. Functional activation is by testing voxelwise hypothesis such as

$$H_0: C\beta = \gamma \text{ vs } H_1: C\beta \neq \gamma.$$

The likelihood is maximized under the unconstrained alternative and under the constrained null hypothesis to produce the below hat and tilde estimates respectively. The generalized likelihood ratio test  $\lambda$  is formed where the ratio of null and alternative hypothesis estimates inserted into the likelihoods of the numerator and denominator respectively. The test statistic  $-2\log\lambda = 2n\log(\tilde{\sigma}^2/\hat{\sigma}^2)$  is formed in each voxel.

$$\hat{\theta} = .5 \tan^{-1} [2\hat{\beta}_R' (X'X)^{-1} \hat{\beta}_I / (\hat{\beta}_R' (X'X)^{-1} \hat{\beta}_R - \hat{\beta}_I' (X'X)^{-1} \hat{\beta}_I)]$$

$$\tilde{\theta} = .5 \tan^{-1} [2\tilde{\beta}_R' \Psi (X'X)^{-1} \tilde{\beta}_I / (\tilde{\beta}_R' \Psi (X'X)^{-1} \tilde{\beta}_R - \tilde{\beta}_I' \Psi (X'X)^{-1} \tilde{\beta}_I)]$$

$$\hat{\beta} = \hat{\beta}_R \cos \hat{\theta} + \hat{\beta}_I \sin \hat{\theta},$$

$$\tilde{\beta} = \Psi (\hat{\beta}_R \cos \tilde{\theta} + \hat{\beta}_I \sin \tilde{\theta}) + (X'X)^{-1} C' [C(X'X)^{-1} C']^{-1} \gamma$$

$$\hat{\sigma}^2 = \{y' - [(X\hat{\beta} \cos \hat{\theta})', (X\hat{\beta} \sin \hat{\theta})']\}' \{y' - [(X\hat{\beta} \cos \hat{\theta})', (X\hat{\beta} \sin \hat{\theta})']\}' / (2n)$$

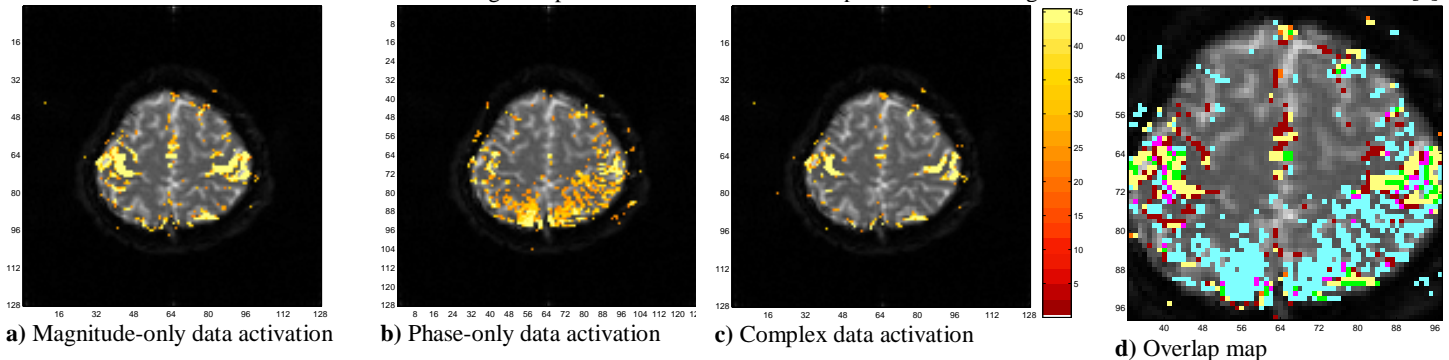
$$\tilde{\sigma}^2 = \{y' - (X\tilde{\beta} \cos \tilde{\theta})', (X\tilde{\beta} \sin \tilde{\theta})']\}' \{y' - [(X\tilde{\beta} \cos \tilde{\theta})', (X\tilde{\beta} \sin \tilde{\theta})']\}' / (2n)$$

$$\hat{\beta}_R = (X'X)^{-1} X' y_R, \quad \hat{\beta}_I = (X'X)^{-1} X' y_I$$

$$\Psi = I_{q+1} - (X'X)^{-1} C' [C(X'X)^{-1} C']^{-1} C$$

## Example:

Single subject data from a block design sequential bilateral finger tapping experiment with 16s off followed by eight epochs of 16s on and 16s off. A 1.5T GE Signa was used single shot full  $k$ -space where 5 axial slices of  $96 \times 96$  acquired reconstructed to  $128 \times 128$ . Voxels were  $1.5625 \times 1.5625$  mm in plane and 5mm thick with  $TE=47$ ms and  $TR=1$ s where  $n=272$  observations taken. The first 3 observations were deleted followed by low frequency and respiration filtering. A single axial slice of data was selected for analysis. The complex regression model was fit with an intercept, time trend, and  $\pm 1$  reference function that mimicked the timing of experiment. Activation was computed with the  $-2\log\lambda$  statistic and Bonferroni thresholded [2].



In **Fig. 1a**) is the map from magnitude-only data, **b**) from phase-only data, **c**) from complex data, and **d**) a zoomed in colored overlap map of above threshold voxels. Note that the complex data activation pattern is more localized with the complex data model than the magnitude-only data model. In **Fig. 1d**), voxels that are only above the threshold for the magnitude-only data model are **red**, only for the phase-only data model **light blue**, only for the complex data model **orange**, for the magnitude-only and phase-only data models **pink**, for the magnitude-only data and complex data models **yellow**, and for all three models **green**. There were no voxels that were above threshold for both the phase-only data model and the complex data model. It can be seen that the **pink** voxels with task related phase changes are below the threshold for the complex data model. A closer inspection of the **red** voxels reveals that they also exhibit task related phase changes. It can be concluded that the magnitude activation from complex data model with a constant phase strongly biases against voxels with task related phase changes which was verified by additional simulations not shown. It was recently shown that voxels containing large vessels exhibit task related changes in both the magnitude and phase whereas voxels with small vessels such as parenchymal tissue only have task related magnitude changes [4].

## Conclusion:

The magnitude-only data, phase-only data, and magnitude activation from complex data with a constant phase models were applied to a real data set. Activation from this complex data model was more focused over the magnitude-only data model and concentrated on voxels without phase changes.

## References:

1. Bandettini, P.M. and Jesmanowicz, A. and Wong, E.C and Hyde, J.S., (1993). Processing strategies for time-course data sets in functional MRI of the human brain. *Magn. Reson. Med.* 30(2):161-173.
2. Logan, B.R. and Rowe, D.B. and (2004). An evaluation of thresholding techniques in fMRI analysis. 22(1):95-108.
3. Rowe, D.B. and Logan, B.R.(2004). A complex way to compute fMRI activation. *NeuroImage.* 23(3):1078-1092.
4. Menon, R.S., (2002). Postacquisition suppression of large-vessel BOLD signals in high-resolution fMRI. *Magn. Reson. Med.* 47(1):1-9.